Chapter 3

Quadratic Gain Bidirectional DC-DC Converter

3.1 Introduction

The designed Quadratic gain bidirectional converter (QGBC) has a simple topology, control strategy, and a large voltage gain, which ensures wide voltage range operation when compared to conventional bidirectional buck or boost converter. The topology of the QGBC shown in Figure 3.1 has four power switches with an anti-parallel diode, two power diodes, two inductors, and two capacitors. The magnitude and direction of the power are controlled by using the QGBC. The QGBC operates in two modes: Motoring (boost) and regenerative braking (buck) mode. The electrical power flows from the battery to the Permanent magnet brushless DC (PMBLDC) motor through VSI in the motoring mode. Simultaneously, the kinetic energy of the PMBLDC motor is converted into electrical energy and fed back to the battery through the bidirectional VSI during the regenerative braking. Regenerative braking can be achieved by reversal of power flow from the battery to the PMBLDC motor.

A brief outline of the chapter is as follows:

- The step-up or motoring mode of operation is discussed in section 3.2.
- The step-down or regenerative braking mode of operation in section 3.3.
- The design parameters of the converter are presented in section 3.4.

- Simulation results and validation through developed prototype are explained in section 3.5 and section 3.6, respectively.

- The conclusion is done in section 3.7.

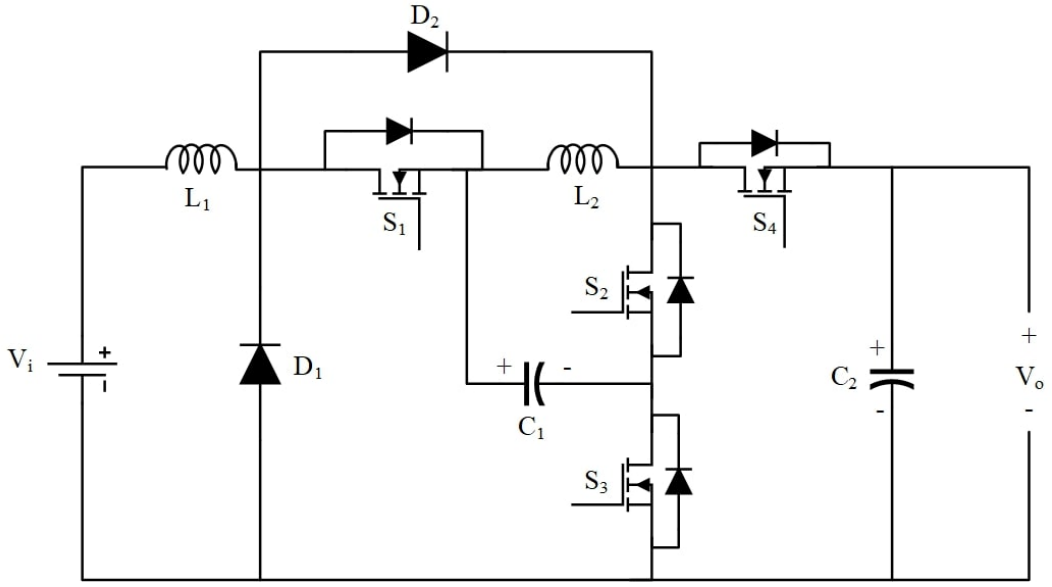

Figure 3.1: The topology of quadratic gain bidirectional DC-DC converter.

3.2 Step-up or Motoring mode of operation

The converter is designed to operate in the continuous inductor current mode (CICM) in steady-state as well as in low load conditions. The capacitors C_1 and C_2 are sufficient to maintain a steady voltage during one period of switching (T_s). In motoring mode operation, the switches S_1 and S_4 are OFF, switch S_3 is always turned ON to avoid switching losses, and switching of switch S_2 is controlled with PWM to execute the boosting operation. The following two modes explain the converter's motoring (boost) mode operation.

3.2.1 Mode 1 (0, T_{on})

The switches S_2, and S_3 are ON for time intervals 0 to DT_s, and S_1 and S_4 are OFF. In this mode, the energy stored in the capacitor C_1 is transferred to the inductor L_2 and the battery voltage V_i charges the inductor L_1, the current flowing path as shown in Figure 3.2.

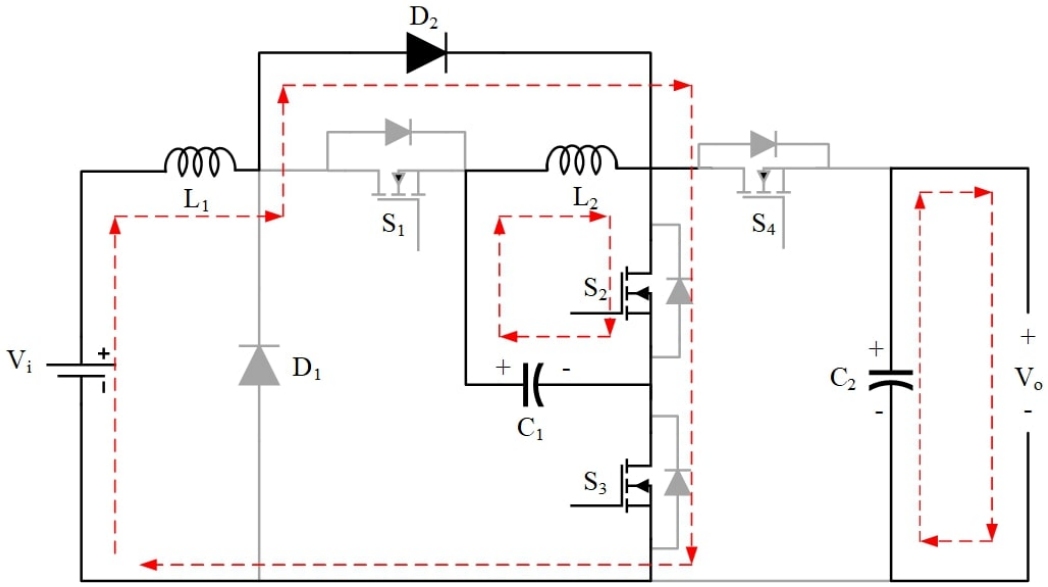

Figure 3.2: Converters' boost mode operation in Mode-1.

The voltage across inductors L_1, L_2 and current through capacitors C_1, C_2 are written as:

$$V_{L1} = V_i \tag{3.1}$$

$$V_{L2} = V_{c1} \tag{3.2}$$

$$i_{c1} = -i_{L2} \tag{3.3}$$

$$i_{c2} = -i_o \tag{3.4}$$

$$i_{L1} = i_s \tag{3.5}$$

3.2.2 Mode 2 (T_{on}, T_s)

In this mode, S_3 is ON, and the rest three switches are OFF for time interval (1-D)T_s. During this mode, the inductor L_2 transfers its stored energy to the DC link capacitor C_2 and capacitor C_1 is being charged by inductor L_1, the current flowing path as shown in Figure 3.3. The voltage and current waveform of converter's boost mode in steady-state is illustrated in Figure 3.4.

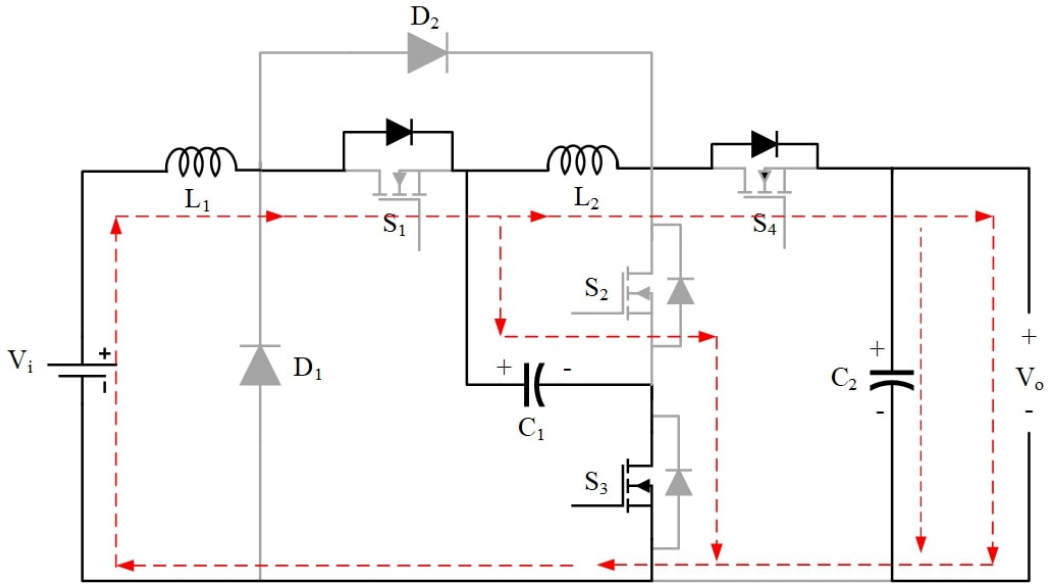

Figure 3.3: Converters' boost mode operation in Mode-2.

The voltage across inductors L_1, L_2 and current through capacitors C_1, C_2 are written as:

$$V_{L1} = V_i - V_{C1} \tag{3.6}$$

$$V_{L2} = V_{C1} - V_o \tag{3.7}$$

$$i_{C1} = i_{L1} - i_{L2} \tag{3.8}$$

$$i_{C2} = i_{L2} - i_o \tag{3.9}$$

For these two modes of boost operation, the volt-sec balance principle across inductors L_1 and L_2 with C_1 at voltage V_{c1} yields the following equations:

$$DT_sV_i + (1-D)T_s(V_i - V_{C1}) = 0 \tag{3.10}$$

$$DT_sV_{C1} + (1-D)T_s(V_{C1} - V_o) = 0 \tag{3.11}$$

By eliminating V_{C1} from (3.10) and (3.11), the voltage gain in boost mode is obtained as:

$$\frac{V_o}{V_i} = \frac{1}{(1-D)^2} \tag{3.12}$$

where $D = T_{on}/T$ is duty ratio and the quadratic nature of the converter can be inferred from (3.12).

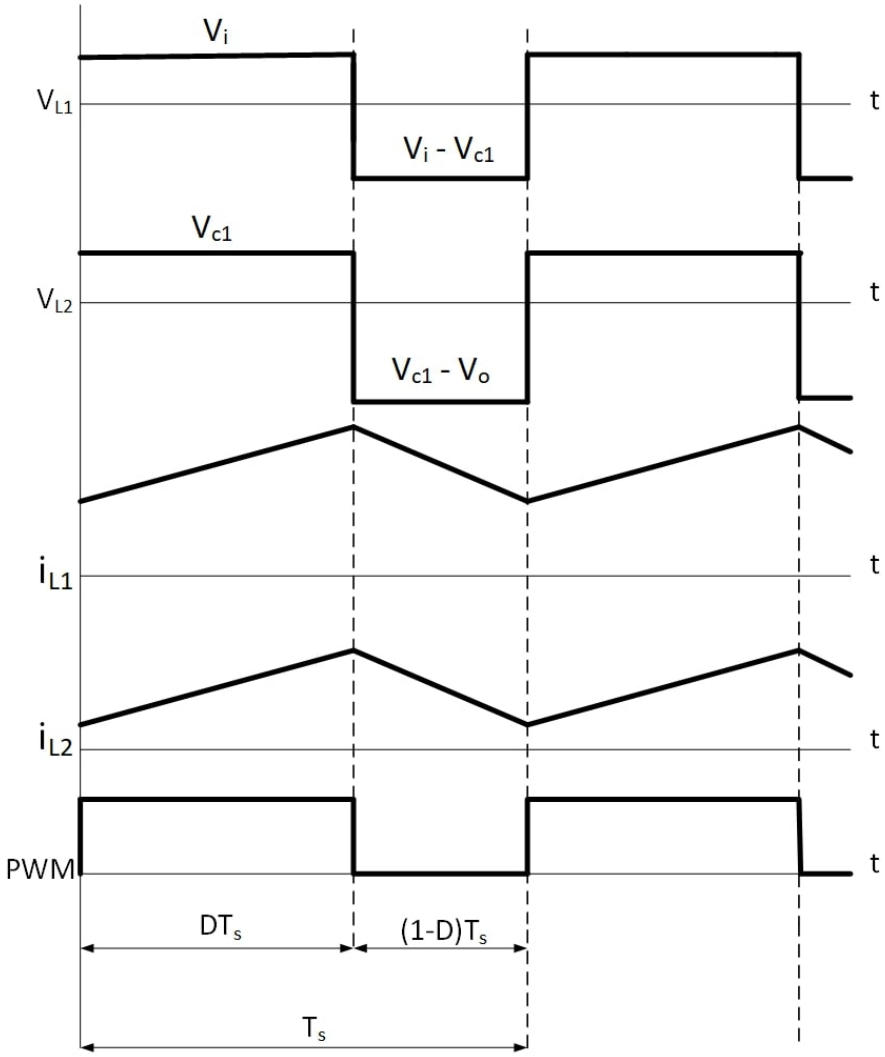

Figure 3.4: Converter's voltage and current waveforms in boost mode.

3.3 Step-down or Regeneartive braking mode of operation

The converter's braking (buck) mode is employed to perform RB, and this allows the mechanical energy stored in the inertial load and the rotor of the PMBLDC motor to be transferred back to the source. In the braking (buck) mode operation, the switches S_1, and S_4 are controlled with PWM simultaneously. The switches S_2 and S_3 are OFF throughout this mode of operation. The braking (buck) mode can be described in two stages of operation. These operations have been explained briefly in subsequent subsections.

3.3.1 Mode 1 (0 , T_{ON})

The switches S_1 and S_4 are ON for the time interval 0 to DT_s in this mode of operation. During this time interval, current in inductor L_1 and L_2 increases, as inductors are being charged by capacitors C_1 and C_2 respectively, the current flowing path of the converter during this mode is shown in Figure 3.5.

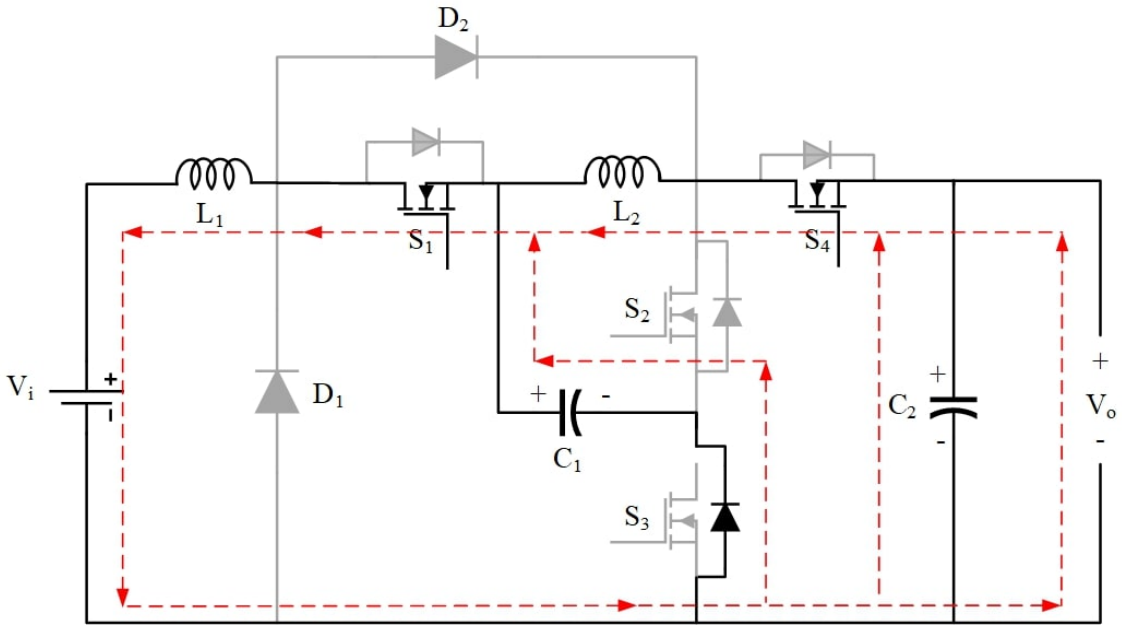

Figure 3.5: Convers' buck mode operation in Mode-1.

The voltage across inductors L_1, L_2 and current through capacitors C_1, C_2 are written as:

$$V_{L1} = V_{C1} - V_i \tag{3.13}$$

$$V_{L2} = V_o - V_{C1} \tag{3.14}$$

$$i_{C1} = i_{L2} - i_{L1} \tag{3.15}$$

$$i_{C2} = i_o - i_{L2} \tag{3.16}$$

3.3.2 Mode 2 (T_{ON}, T_s)

All the switches S_1, S_2, S_3, and S_4 are OFF for the time interval (1-D)T_s. The stored energy of inductor L_1 is transferred to the battery at voltage V_i and energy of inductor L_2 to capacitor C_1. The load at voltage V_o is feeding the regenerated energy to capacitor C_2, the conduction path of the converter in this mode is shown in Figure 3.6.

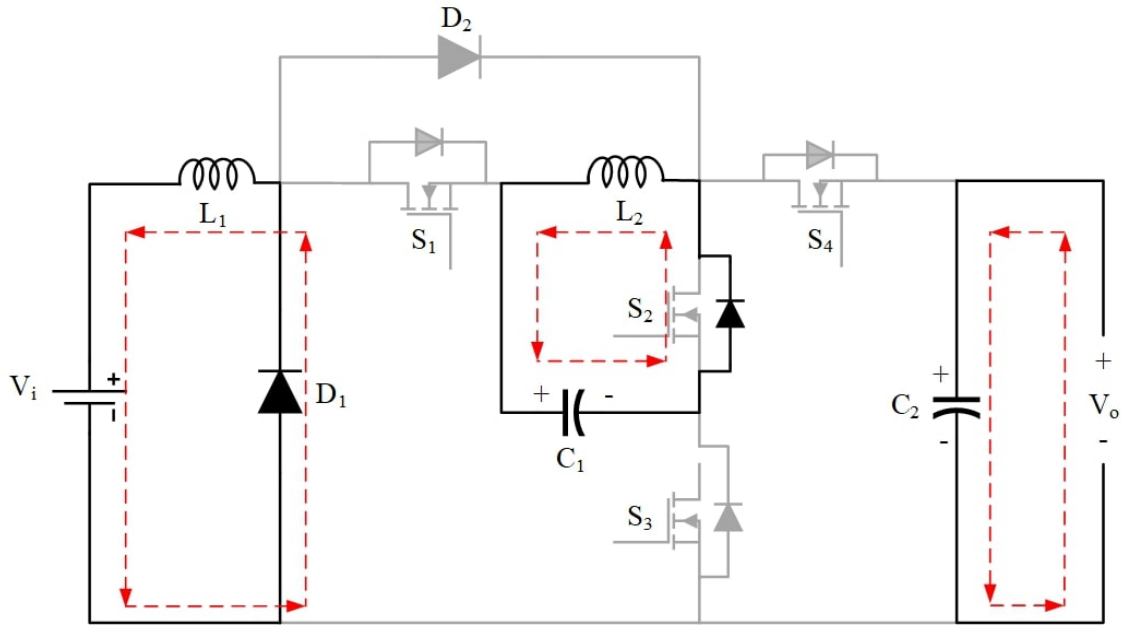

Figure 3.6: Converter's buck mode operation in Mode-2.

The waveforms of inductor currents and voltages are depicted in Figure 3.7. The voltage across inductors L_1, L_2 and current through capacitors C_1, C_2 are written as:

$$V_{L1} = V_i \tag{3.17}$$

$$V_{L2} = V_{C1} \tag{3.18}$$

$$i_{C1} = i_{L2} \tag{3.19}$$

$$i_{C2} = i_o \tag{3.20}$$

For these two modes of buck operation, the volt-sec balance principle across inductors L_1 and L_2 with C_1 at voltage V_{c1} yields the following equations:

$$D(V_i - V_{C1}) + (1 - D)V_i = 0 \tag{3.21}$$

$$D(V_{C1} - V_o) + (1 - D)V_{C1} = 0 \tag{3.22}$$

By eliminating V_{C1} from (3.21) and (3.22), the voltage gain in buck mode is obtained as:

$$\frac{V_i}{V_o} = D^2 \tag{3.23}$$

The voltage gain in buck mode is quadratic in nature.

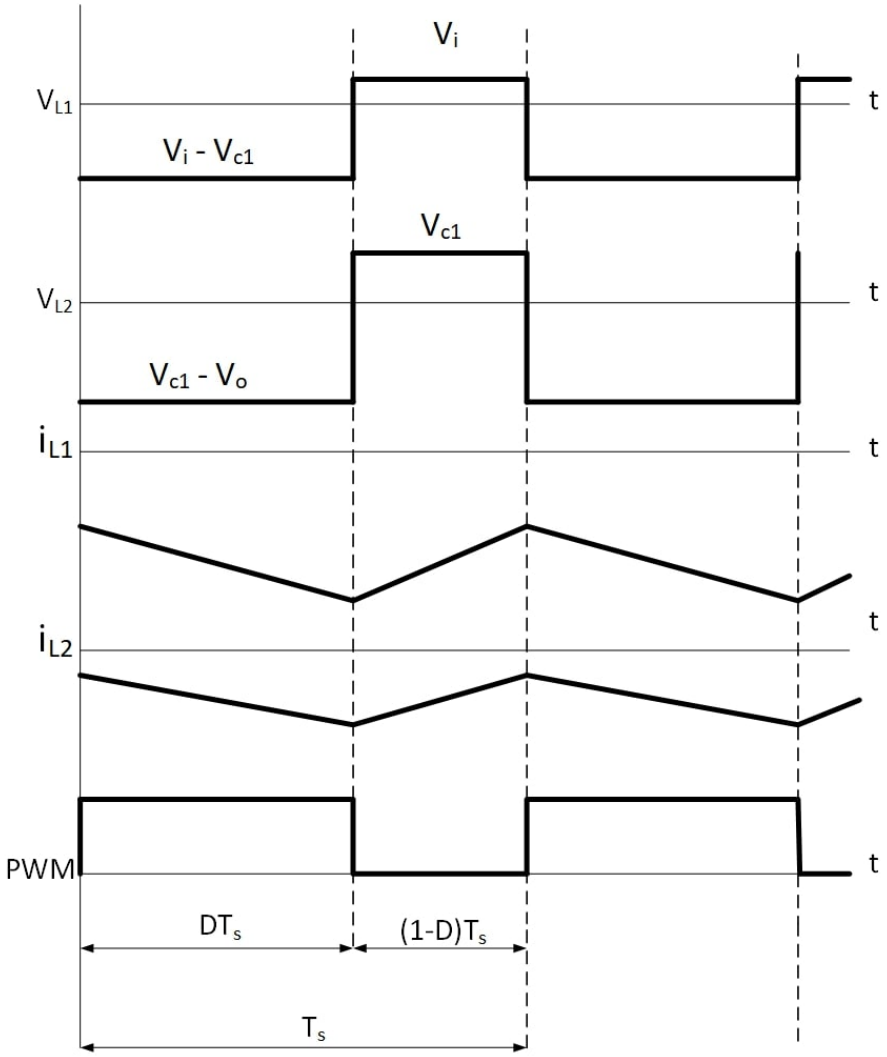

Figure 3.7: Converter's voltage and current waveform in buck mode.

3.3.3 Regenerative braking commutation by three switch strategy

Power resistors have been used for conventional dynamic braking, where the kinetic energy of an electric machine is dissipated through armature winding and additional braking resistance. The principle of regenerative braking is similar to conventional dynamic braking; however, additional resistance is eliminated and the kinetic energy of the vehicle can be recovered. The PMBLDC machine will act as generator during regenerative braking. The back-Electromotive force (EMF), armature current of all three phase and equivalent circuit of PMBLDC motor are illustrated in Figure 3.8. In the three switch strategy, low side power transistor T_2, T_4, and T_6 are operated in synchronous PWM switching mode

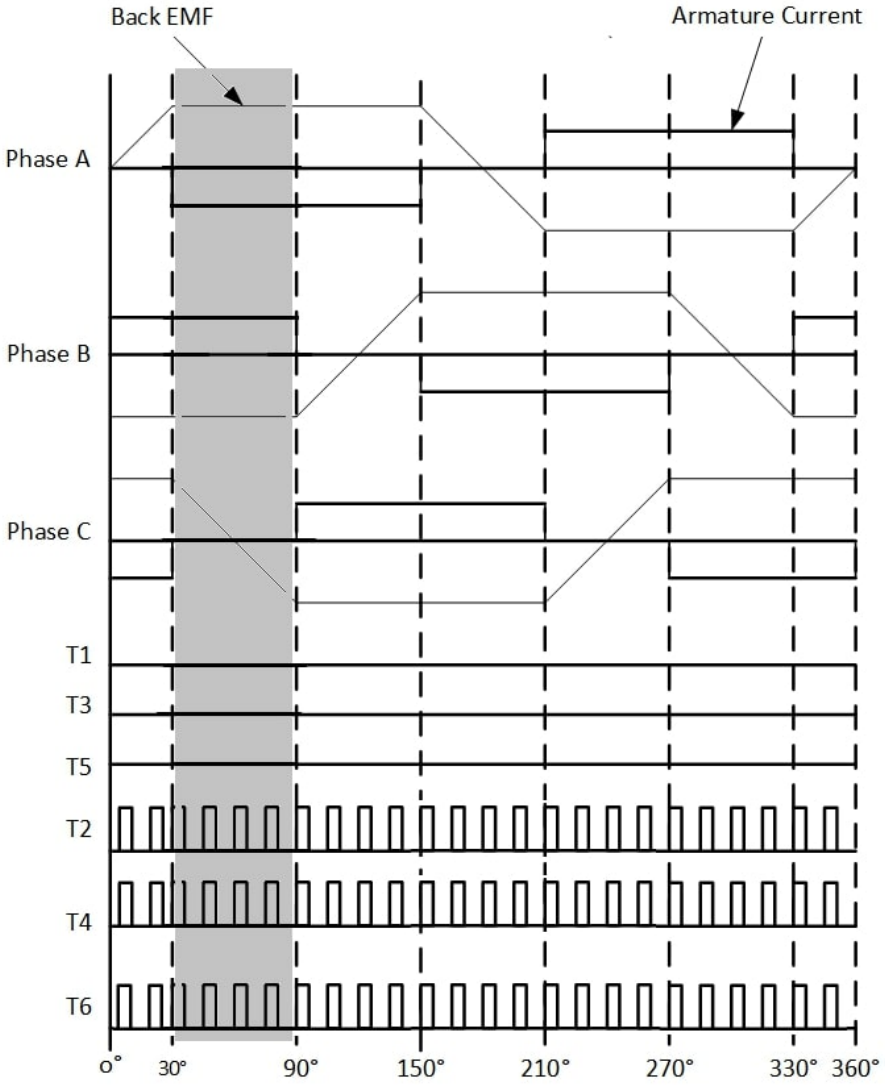

(a)

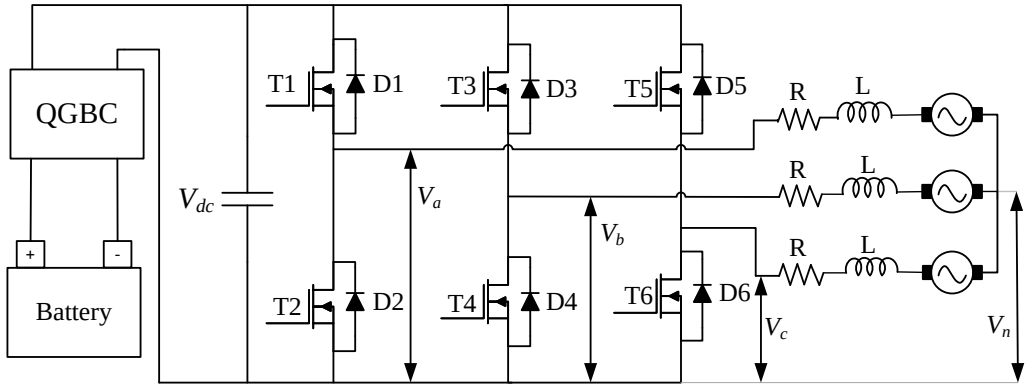

(b)

Figure 3.8: The working waveform of PMBLDC motor and Equivalent circuit for three-switch strategy (a) Back-EMF, armature current and switching signal of PMBLDC motor (b) Bidirectional VSI with equivalent circuit of a PMBLDC motor.

in each electric cycle, in which the electric machine can generate torque while simultaneously recovering energy. One interesting observation of the PMBLDC motor is that the back-EMF of each phase has a sign change at an interval of 30 electrical degrees. The back-EMF is positive in phase c from 30 to 60 electrical degrees, whereas the back-EMF is negative in phase c from 60 to 90 electrical degrees. As a result, the following analysis is performed for every 30 electrical degrees. The average circuit parameter values (e.g. resistance, inductance) for these two equivalent circuits will be used to describe the characteristics of the PMBLDC motor using the three-switch strategy. The current paths of the PMBLDC motor in 30 and 60 electrical degrees operating states are shown in Figure 3.9.

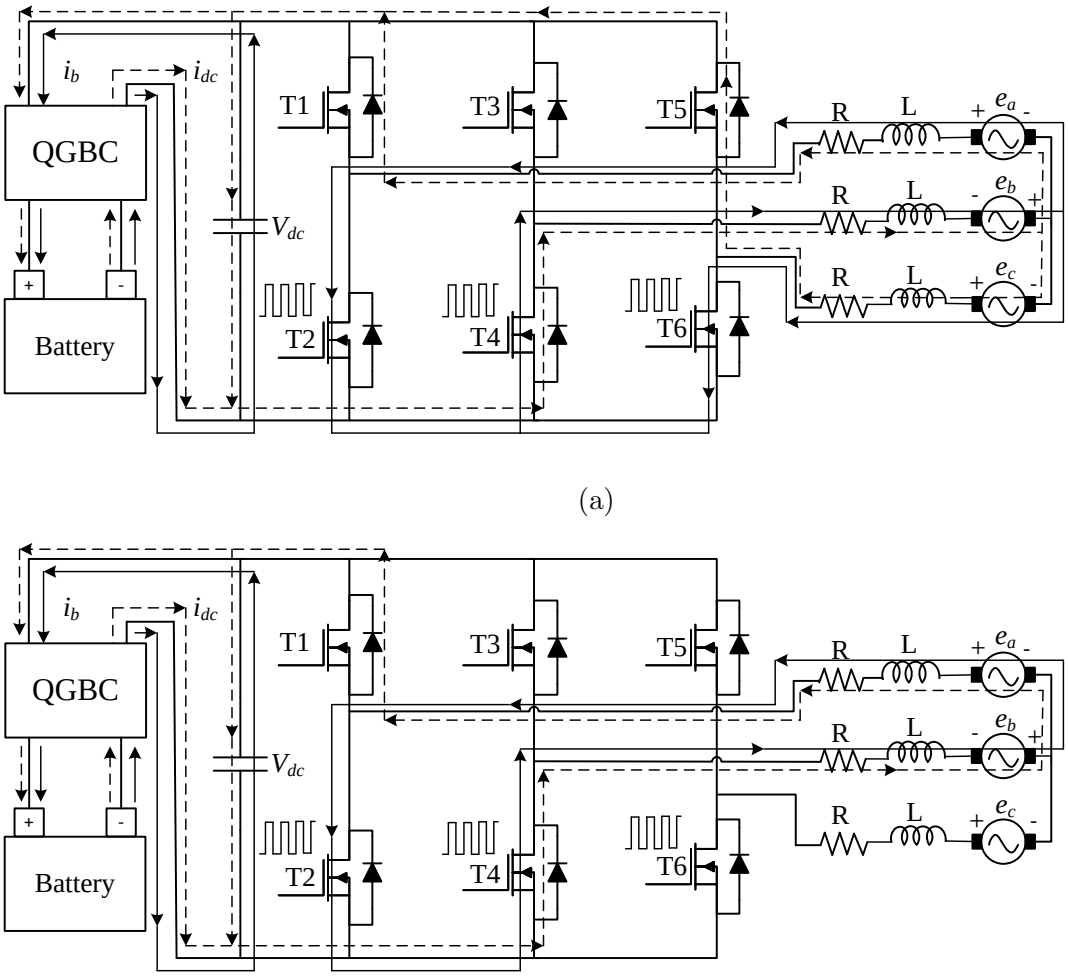

(a)

(b)

Figure 3.9: Current flowing path of three-switch strategy (solid line: switches are ON; dotted line: switches are OFF) (a) At 30 electrical degree and (b) At 60 electrical degree.

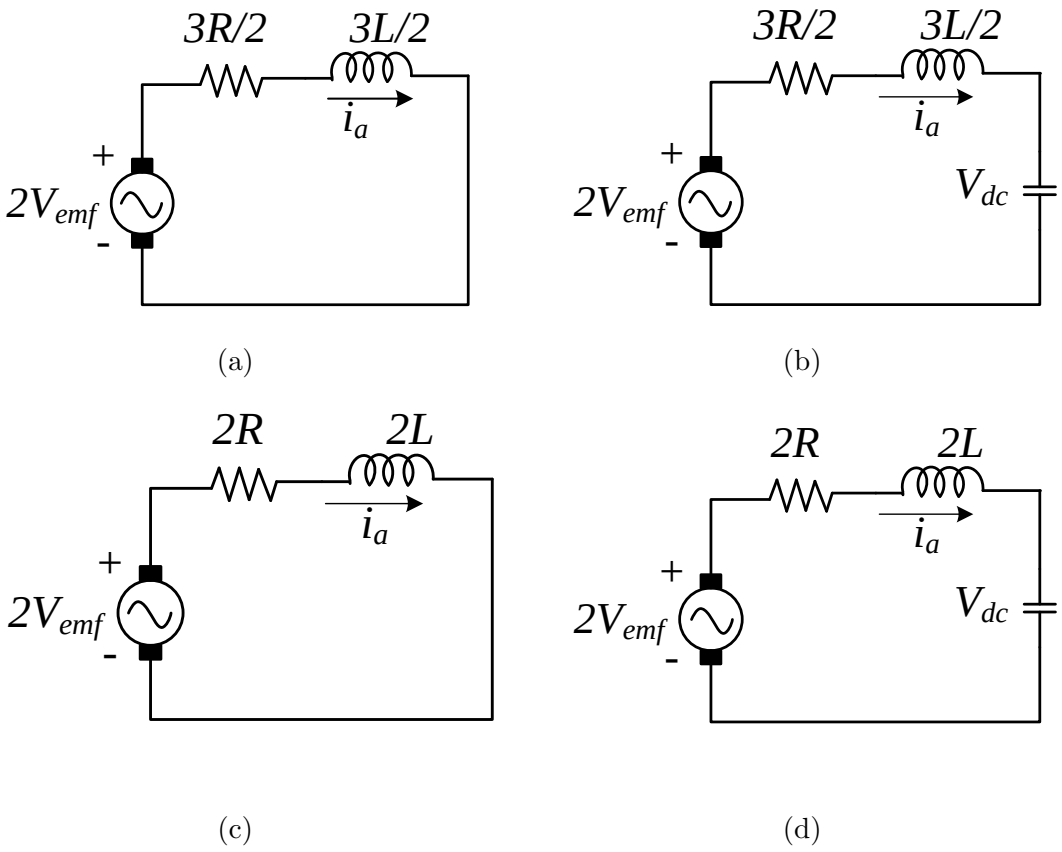

Figure 3.10: Equivalent cicuits of PMBLDC motor using three-switch strategy at 30 and 60 electrical degree (a) ON state at 30^o, (b) OFF state at 30^o, (c) ON state at 60^o and (d) OFF state at 60^o.

The equivalent circuits of the PMBLDC motor using three-switch strategy are shown in Figure 3.10. Now applying volt-second and charge-second principle on equivalent inductor L and dc link capacitor, the following equation are obtained:

$$\delta T[2V_{emf} - i_a(\frac{7}{4}R)] + \delta^{'}T[2V_{emf} - i_a(\frac{7}{4}R) - V_{dc}] = 0 \tag{3.24}$$

$$\delta T(-\frac{V_{dc}}{R_e}) + \delta^{'}T(i_a - \frac{V + dc}{R_e}) = 0 \tag{3.25}$$

where R_e is the equivalent resistance of switches in QGBC and battery, δ is duty ratio of switching PWM, T is switching time period and $\delta^{'}$=(1-δ). On solving (3.24) and (3.25), the average armature current and dc link voltage is obtained as:

$$i_a = \frac{2V_{emf}}{(\delta^{'2}R_e + (7/4)R)} \tag{3.26}$$

$$V_{dc} = \frac{2V_{emf}}{(\delta^{'} + (7/4)(K/\delta^{'}))} \tag{3.27}$$

The voltage ratio is derived as:

$$\frac{V_{dc}}{V_{emf}} = \frac{2}{(\delta' + \frac{7K}{4\delta'})} \tag{3.28}$$

where $K = R/R_e$. The voltage ratio equation can be used to determine kinetic energy recovered when speed and other parameters of the PMBLDC motor are known. The regenerative braking of the PMBLDC motor with a three-switch strategy is easy since the rotor position information is not required. The three-switch strategy can produce enough braking torque in medium to high speed region.

3.4 Converter Design and Stability Analysis

3.4.1 Converter Design

The converter design is done as per the boost and buck operations, as explained in Figure 3.4 and Figure 3.7. The designed converter is thus operated in the CICM, and the output capacitor value is selected for minimum output voltage ripple. The inductor values are calculated to keep the converter in CICM operation even at low load conditions. The duty ratio (D) is calculated as 30% for an output voltage of 98 V with an input battery voltage of 48 V. Switching frequency (f_s) of the converter is 15 kHz. The minimal load for the PMBLDC motor constitutes the switching losses in VSI, copper, iron, and windage losses. Thus, a minimal burden of 40 W is considered for calculations.

$$V_{co} = V_o = \frac{V_i}{(1-D)^2} \tag{3.29}$$

$$V_i \times I_{L1} = V_o \times I_o \tag{3.30}$$

No load power = 40 W

$$I_{L1} = \frac{P_{min}}{V_i} = 0.8\text{A} \tag{3.31}$$

$$\Delta I_{L1} = 1.6\text{A} \tag{3.32}$$

$$V_i = L_1 \times \frac{\Delta I_{L1}}{DT_s} \tag{3.33}$$

Thus, using (3.33) the value of input inductor L_1 is calculated as 0.6 mH. Thus for CICM operation, a higher value of inductance i.e. 1 mH, is selected in this work. The calculation for L_2 is done as follows:

$$I_{L1} = \frac{I_o}{(1-D)^2} \tag{3.34}$$

$$I_{L2} = \frac{I_o}{(1-D)} \tag{3.35}$$

The calculated value of I_{L2} at minimum load is 0.56 A thus the current ripple at boundary condition operation is 1.12 A.

$$V_{c1} = \frac{V_i}{(1-D)} \tag{3.36}$$

$$V_{c1} = L_2 \times \frac{\Delta I_{L2}}{DT_s} \tag{3.37}$$

The value of Inductor L_2 is calculated by using (3.37) as 1.2 mH. Thus for CICM operation a higher value of 1.5 mH is selected in this work. The calculation for C_1 is as follows:

$$I_c = C_1 \times \frac{dV_{c1}}{dt} \tag{3.38}$$

$$I_c = -L_{L2} \tag{3.39}$$

$$I_{L2} = C_1 \times \frac{\Delta V_{c1}}{DT_s} \tag{3.40}$$

Taking $\Delta\ V_{c1} = 10\ \%$ of V_{c1}, The value of capacitor C_1 is calculated as 43 μF. The readily available 47 μF value is selected in this work.

$$I_{co} = C_2 \times \frac{dV_{co}}{dt} \tag{3.41}$$

$$I_{L2} - I_o = C_2 \times \frac{\Delta V_{co}}{(1-D)T_s} \tag{3.42}$$

For the value of $\Delta\ V_{co} = 2\ \%$ of V_{co} and $f_s = 15$ kHz, the value of C_2 is calculated as 102 μF. The commercially available capacitor with a higher value of 220 μF is selected for this work.

The value of passive components of the converter for buck mode operation is calculated in a similar way as in boost mode operation since the no-load power is the same in boost or buck operation. With V_o= 98 V and V_i= 48 V then the duty cycle is calculated as

D=0.7 and switching frequency of 15 kHz.

$$V_i = D^2 V_o \tag{3.43}$$

$$V_i \times I_{L1} = V_o \times I_o \tag{3.44}$$

$$I_{L1} = I_i \tag{3.45}$$

$$I_o = D^2 I_i \tag{3.46}$$

No load power = 40 W

$$I_o = \frac{P_o}{V_o} = 0.408\text{A} \tag{3.47}$$

$$I_{l1} = 0.816\text{A} \tag{3.48}$$

$$\Delta I_{L1} = 1.63\text{A} \tag{3.49}$$

$$L_1 \frac{\Delta I_{L1}}{DT_s} = V_{C1} - V_i \tag{3.50}$$

The value of inductor L_1 is calculated by using (3.50) as 0.58 mH. The calculation for L_2 is done as follows:

$$I_{L2} = DI_{L1} \tag{3.51}$$

$$\Delta I_{L2} = 1.141\text{A} \tag{3.52}$$

$$L_2 \frac{\Delta I_{L2}}{DT_s} = V_o - V_{C1} \tag{3.53}$$

The value of inductor L_2 is calculated by using (3.53) as 1.19 mH. The calculation for C_1 is done as follows:

$$I_{C1} = I_{L1} - I_{L2} = C_1 \frac{\Delta V_{C1}}{DT_s} \tag{3.54}$$

After substituting the value of $\Delta\ V_{C1}$=10% of V_{c1}, D and T_s. The value of C_1 is calculated as 2 μ F. The calculation for C_2 is done as follows:

$$I_{L2} - I_o = C_2 \frac{\Delta V_{co}}{DT_s} \tag{3.55}$$

For the value of $\Delta\ V_{co}$= 2% of V_{co} and f_s = 15 kHz, The value of C_2 is calculated as 4 μ F. The calculated values of passive components in buck mode of operation are lower than that of boost mode operation. Hence, the converter is designed as per the boost mode

values and the calculation for the boost mode is included in the chapter. The voltage stress on switches S_1, S_2, S_3, and S_4 are calculated as:

$$V_{S1} = \frac{V_s}{(1-D)} \tag{3.56}$$

$$V_{S2} = \frac{V_s}{(1-D)^2} \tag{3.57}$$

$$V_{S3} = \frac{V_s}{(1-D)} \tag{3.58}$$

$$V_{S4} = \frac{V_s}{(1-D)^2} \tag{3.59}$$

stress on switches is low as compared to the converter in [120] and [89]. The converter is designed as per the designated parameters are given in Table 3.1. The calculated converter passive elements are given Table 3.2.

Table 3.1: Converter specifications

Parameter	Value
Input Voltage(V_i)	48 V
Output Power(P_o)	1000 W
Output Voltage(V_o)	98 V
Operating Frequency (f_s)	$15KHz$

Table 3.2: Converter passive components

Converter Parameter	Value
Inductor 1 (L_1)	1 mH
Inductor 2 (L_2)	1.5 mH
Capacitor 1 (C_1)	47 μF
Capacitor 2 (C_2)	220 μF
Switches S_1-S_4	STWA63N65DM2
Diode D_1, D_2	FFSH3065A

3.4.2 Small-signal Analysis

The dynamic analysis of the proposed converter is based on the small perturbation theory. Dynamic equations of the converter are linearized around the operating points as follows:

$$\dot{x}(t) = Ax + Bu \tag{3.60}$$

$$y(t) = Cx + Du \tag{3.61}$$

where x is the space state vector, u is the input vector, and y is the output vector. The dynamic equation of the converter step-up during Mode-1 operation is written as

$$-V_s + L_1 \frac{di_{L1}}{dt} = 0 \tag{3.62}$$

$$L_2 \frac{di_{L2}}{dt} - V_c = 0 \tag{3.63}$$

$$C_1 \frac{dV_{c1}}{dt} + i_{L2} = 0 \tag{3.64}$$

$$C_2 \frac{dV_{c2}}{dt} + i_o = 0 \tag{3.65}$$

$$V_o = V_{c2} \tag{3.66}$$

The above dynamic equation is rewritten in the form of state space as follow:

$$\dot{x}(t) = A_1 x + B_1 u \tag{3.67}$$

$$\begin{pmatrix} \dot{i_{L1}} \\ \dot{i_{L2}} \\ \dot{v_{c1}} \\ \dot{v_{c2}} \end{pmatrix} = \begin{pmatrix} 0 & 0 & 0 & 0 \\ 0 & 0 & \frac{1}{L_2} & 0 \\ 0 & -\frac{1}{C_1} & 0 & 0 \\ 0 & 0 & 0 & \frac{-1}{R_o C_2} \end{pmatrix} \begin{pmatrix} i_{L1} \\ i_{L2} \\ v_{c1} \\ v_{c2} \end{pmatrix} + \begin{pmatrix} \frac{1}{L_1} \\ 0 \\ 0 \\ 0 \end{pmatrix} \begin{pmatrix} v_i \end{pmatrix} \tag{3.68}$$

$$y(t) = C_1 x + D_1 u \tag{3.69}$$

$$\begin{pmatrix} v_o \end{pmatrix} = \begin{pmatrix} 0 & 0 & 0 & 1 \end{pmatrix} \begin{pmatrix} i_{L1} \\ i_{L2} \\ v_{c1} \\ v_{c2} \end{pmatrix} + \begin{pmatrix} 0 \end{pmatrix} \begin{pmatrix} v_i \end{pmatrix} \tag{3.70}$$

The dynamic equation of the converter step-up during Mode-2 operation is written as

$$-V_s + L_1\frac{di_{L1}}{dt} + V_{c1} = 0 \tag{3.71}$$

$$L_2\frac{di_{L2}}{dt} + V_{c2} - V_{c1} = 0 \tag{3.72}$$

$$C_1\frac{dV_{c1}}{dt} - i_{L1} + i_{L2} = 0 \tag{3.73}$$

$$C_2\frac{dV_{c2}}{dt} + -i_{L2} + i_o = 0 \tag{3.74}$$

$$V_o = V_{c2} \tag{3.75}$$

The above dynamic equation is rewritten in the form of state space as follow:

$$\dot{x}(t) = A_2x + B_2u \tag{3.76}$$

$$\begin{pmatrix} \dot{i_{L1}} \\ \dot{i_{L2}} \\ \dot{v_{c1}} \\ \dot{v_{c2}} \end{pmatrix} = \begin{pmatrix} 0 & 0 & \frac{1}{L_1} & 0 \\ 0 & 0 & \frac{1}{L_2} & \frac{-1}{L_2} \\ \frac{1}{C_1} & -\frac{1}{C_1} & 0 & 0 \\ 0 & \frac{-1}{C_2} & 0 & \frac{-1}{R_oC_2} \end{pmatrix} \begin{pmatrix} i_{L1} \\ i_{L2} \\ v_{c1} \\ v_{c2} \end{pmatrix} + \begin{pmatrix} \frac{1}{L_1} \\ 0 \\ 0 \\ 0 \end{pmatrix} \begin{pmatrix} v_i \end{pmatrix} \tag{3.77}$$

$$y(t) = C_2x + D_2u \tag{3.78}$$

$$\begin{pmatrix} v_o \end{pmatrix} = \begin{pmatrix} 0 & 0 & 0 & 1 \end{pmatrix} \begin{pmatrix} i_{L1} \\ i_{L2} \\ v_{c1} \\ v_{c2} \end{pmatrix} + \begin{pmatrix} 0 \end{pmatrix} \begin{pmatrix} v_i \end{pmatrix} \tag{3.79}$$

Now applying state-space averaging technique

$$A = A_1D + A_2(1-D) \tag{3.80}$$

$$B = B_1D + B_2(1-D) \tag{3.81}$$

$$A = \begin{pmatrix} 0 & 0 & \frac{-(1-D)}{L_1} & 0 \\ 0 & 0 & \frac{1}{L_2} & \frac{-(1-D)}{L_2} \\ \frac{(1-D)}{C_1} & \frac{-1}{C_1} & 0 & 0 \\ 0 & \frac{-(1-D)}{C_2} & 0 & \frac{-1}{R_oC_2} \end{pmatrix} \tag{3.82}$$

$$B = \begin{pmatrix} \frac{1}{L_1} \\ 0 \\ 0 \\ 0 \end{pmatrix} \tag{3.83}$$

$$C = \begin{pmatrix} 0 & 0 & 0 & 1 \end{pmatrix} \tag{3.84}$$

$$D = \begin{pmatrix} 0 \end{pmatrix} \tag{3.85}$$

Small signal model is derived by applying perturbations, the overall state and output equation of the converter is obtained as

$$\begin{pmatrix} \widetilde{i_{L1}} \\ \widetilde{i_{L2}} \\ \widetilde{v_c} \\ \widetilde{v_{co}} \end{pmatrix} = \begin{pmatrix} 0 & 0 & \frac{-(1-D)}{L_1} & 0 \\ 0 & 0 & \frac{1}{L_2} & \frac{-(1-D)}{L_2} \\ \frac{(1-D)}{C_1} & \frac{-1}{C_1} & 0 & 0 \\ 0 & \frac{-(1-D)}{C_2} & 0 & \frac{-1}{R_o C_2} \end{pmatrix} \begin{pmatrix} \widetilde{i_{L1}} \\ \widetilde{i_{L2}} \\ \widetilde{v_c} \\ \widetilde{v_{c2}} \end{pmatrix} + \begin{pmatrix} \frac{V_{c1}}{L_1} & \frac{1}{L_1} \\ \frac{V_{c2}}{L_2} & 0 \\ \frac{-I_{L1}}{C_1} & 0 \\ \frac{I_{L2}}{C_2} & 0 \end{pmatrix} \begin{pmatrix} \widetilde{d} \\ \widetilde{v_i} \end{pmatrix} \tag{3.86}$$

The perturbation $\widetilde{v_i}$ is assumed to be zero in input voltage to simplify the analysis, which gives v_i=V_i. After substituting all passive elements value from Table 3.2 and duty cycle D = 0.3, the control to output transfer function $G_d(s)$ is obtained as follows:

$$G_d(s) = \frac{\widetilde{v_o(s)}}{\widetilde{d(s)}} = \frac{-7.37 \times 10^4 s^3 + 2.378 \times 10^8 s^2 - 5.88 \times 10^{12} s + 5.1 \times 10^{15}}{1.16 s^4 + 5.5 \times 10^2 s^3 + 3.07 \times 10^7 s^2 + 1.37 \times 10^{10} s + 1.9 \times 10^{13}} \tag{3.87}$$

The poles of the transfer function have negative real part (left half of the s-plane) indicating that system is stable. To improve the steady-state behaviour of the converter, a PI controller is used. Transfer function of a PI controller is

$$G_{PI} = \frac{K_p s + K_i}{s} \tag{3.88}$$

Ziegler-Nicolous' closed loop method is used to tune the PI controller, the value of $K_p = 1.86 \times 10^{-3}$ and $K_i = 0.44$ substituted in (3.88) and therefore the closed-loop transfer function (CLTF) of the converter is obtained as follows

$$\frac{\widetilde{v_o(s)}}{\widetilde{v_{ref}(s)}} = \frac{-1.356 \times 10^2 s^4 + 4.05 \times 10^5 s^3 - 5.197 \times 10^9 s^2 + 8.117 \times 10^{12} s + 2.244 \times 10^{15}}{1.16 s^4 + 5.5 \times 10^2 s^3 + 3.07 \times 10^7 s^2 + 1.37 \times 10^{10} s + 1.9 \times 10^{13}} \tag{3.89}$$

The magnitude and phase plot is obtained from CLTF are shown in Figure 3.11. One can see that the gain margin of 5.4 dB and phase margin of 53.2 degree.

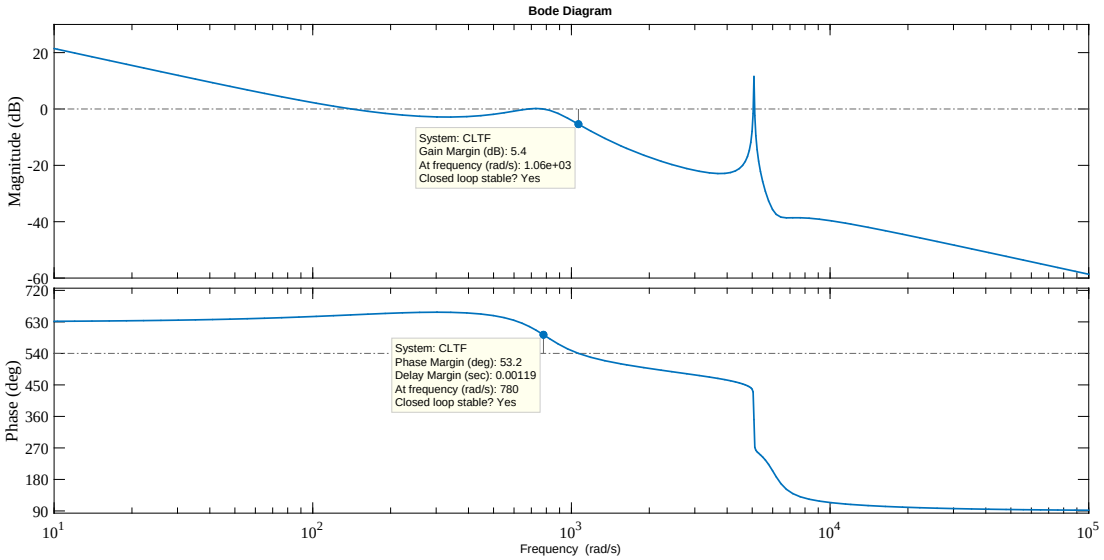

Figure 3.11: Magnitude and Phase plot obtained from CLTF.

3.5 Simulation Results

The bidirectional quadratic converter and VSI fed PMBLDC motor are simulated using MATLAB/Simulink software package. The PMBLDC motor is coupled with an inertial load of 0.1 kg-m^2 thruogh belt. The system is simulated for 7 seconds with 0s to 5s in motoring mode and 5s to 7s in regenerative mode. The intended regenerative action is observed as per the simulation results shown in this chapter. The steady-state inductor currents with a gate driving signal in the converter's boost mode operation are shown in Figure 3.12.

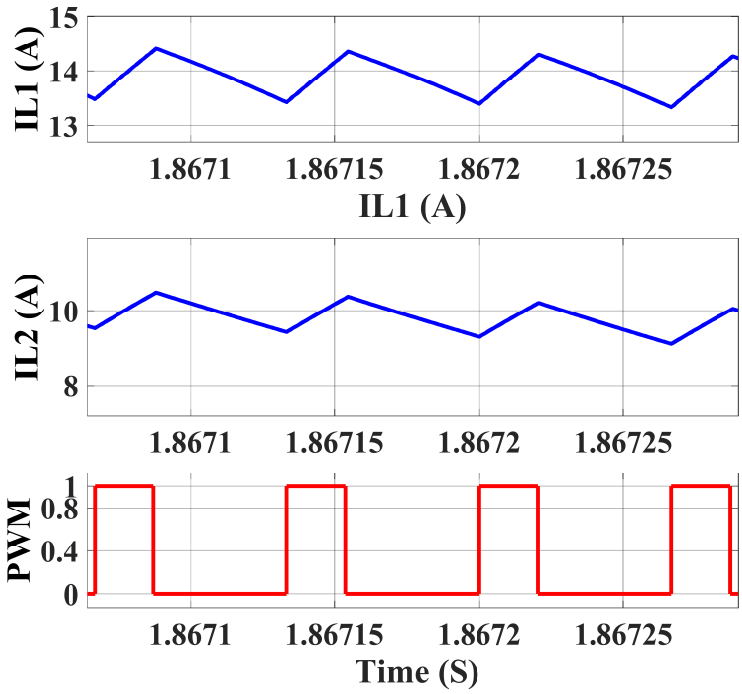

Figure 3.12: Inductor currents I_{L1} and I_{L2} with switching PWM during boost mode.

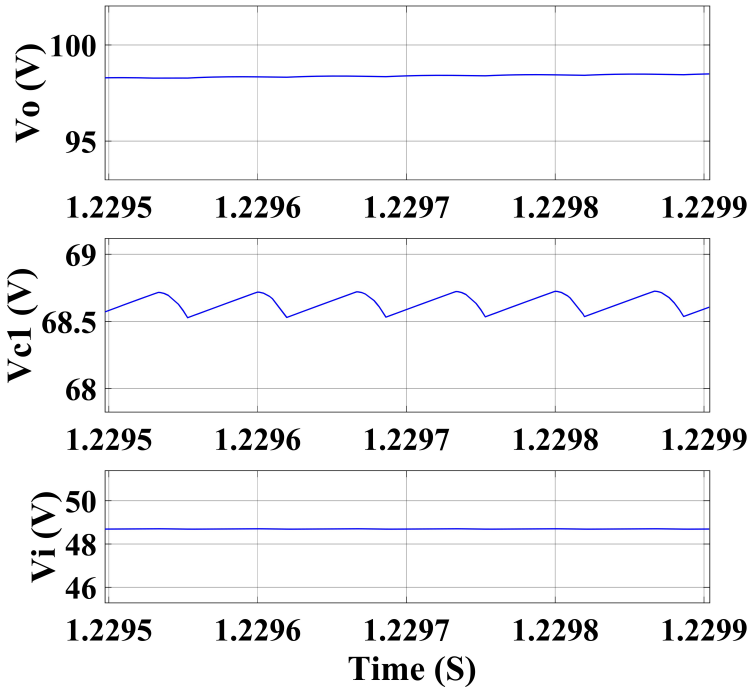

Figure 3.13: Output voltage V_o, Capacitor Voltage V_{c1} and Battery voltage V_i during boost mode.

In boost mode, when the switch is ON, both inductor's current increases, and when the switch is OFF, both inductor's current decreases. In steady-state, the average value of

current I_{L1} is 14 A, and current I_{L2} is 10 A, as shown in Figure 3.12. Figure 13 presents the steady-state output voltage (V_o), voltage (V_{c1}) of capacitor C_1, and battery voltage (V_i) in boost (motoring) mode operation. In boost mode, the steady-state output voltage V_o is 98 V, and capacitor (C_1) voltage V_{c1} is 68.5 V with battery voltage V_i of 48 V at 30% duty ratio, which is shown in Figure 3.13. The battery voltage (V_i) and State of Charge (SOC) are shown in Figure 3.14. It is depicted that during motoring (boost) mode, the battery SOC decreases, and a dip in battery voltage is observed during 0 to 5s of simulation. At t = 5s, regenerative braking is applied, then the converter starts to operate in buck mode, and battery voltage and SOC increase. In buck (regenerative braking) mode, the steady-state inductor currents are I_{L1}= -5 A and I_{L2}= -4 A, respectively. The negative value of inductor currents means the current is flowing from load to source as shown in Figure 3.15.

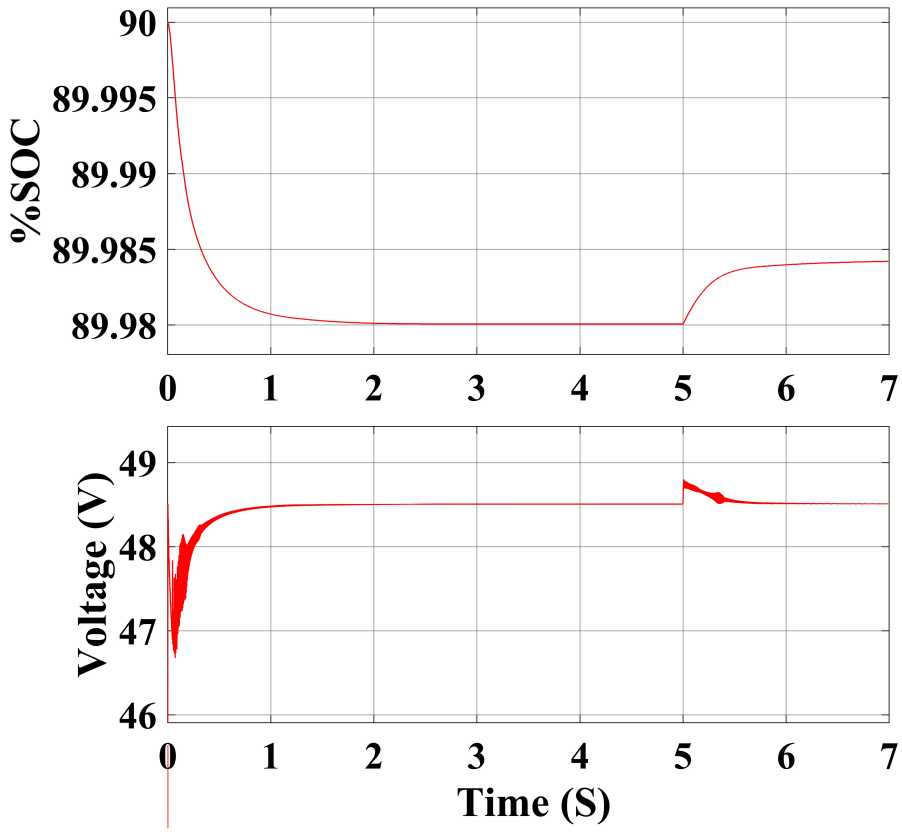

Figure 3.14: Battery voltage and %SOC during motoring and regenerative braking.

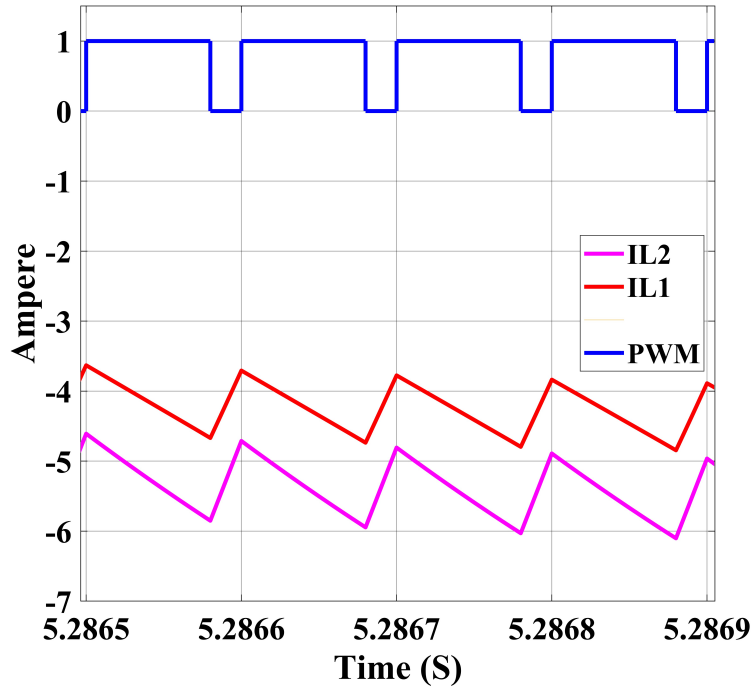

Figure 3.15: Inductor current I_{L1} and I_{L2} with switching PWM during regenerative braking.

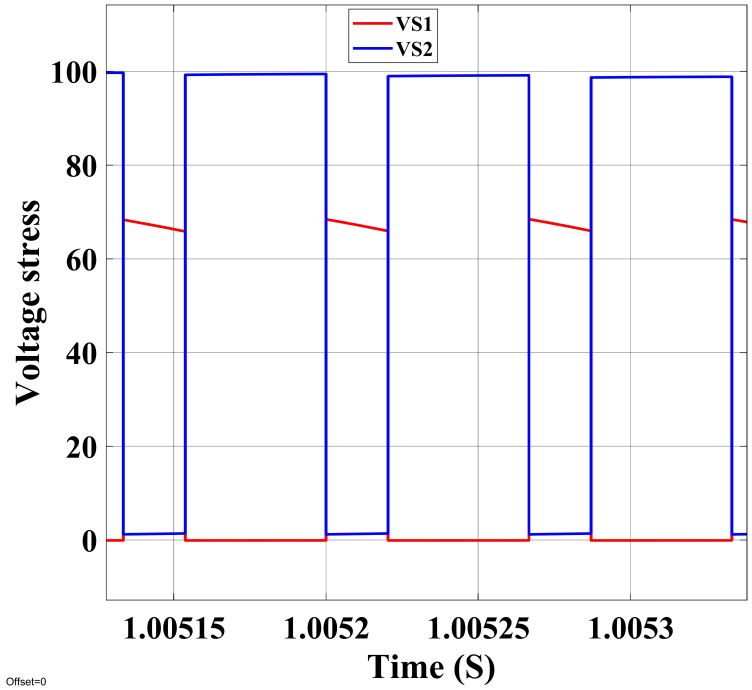

Figure 3.16: Voltage stress on switches S_1 and S_2 during boost mode operation of converter.

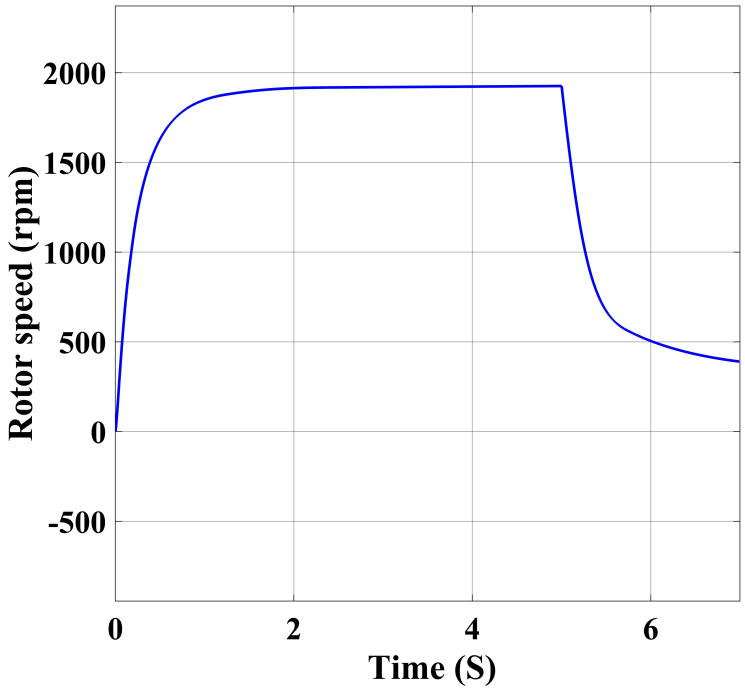

Figure 3.17: Motor speed characteristics during motoring and regenerative braking.

Figure 3.16 shows the voltage stress on switches S_1 and S_2 during boost mode operation of the converter. Motor speed in boost mode reached 2000 rpm from time 0s to 5s. At 5s, regenerative braking is applied, the motor speed starts to decrease in braking mode and reaches 650 rpm at 7s as shown in Figure 3.17.

3.6 Validation through developed prototype

An experimental setup is developed to test the proposed system and the converter prototype. The system employs a 1.1 hp PMBLDC motor coupled with an inertia of the flywheel (J= 0.1 kg-m^2). TMS320F28335 DSP microcontroller controls the developed DC-DC converter and the VSI in both the motoring and regenerative mode. Figure 3.18 shows the setup for the experimental verification of the proposed system. A PMBLDC motor coupled with a high inertia flywheel is used to emulate the load. To reduce the impulse torque condition and safety of the system, a pulley belt system is employed for mechanical coupling of the motor and inertial load.

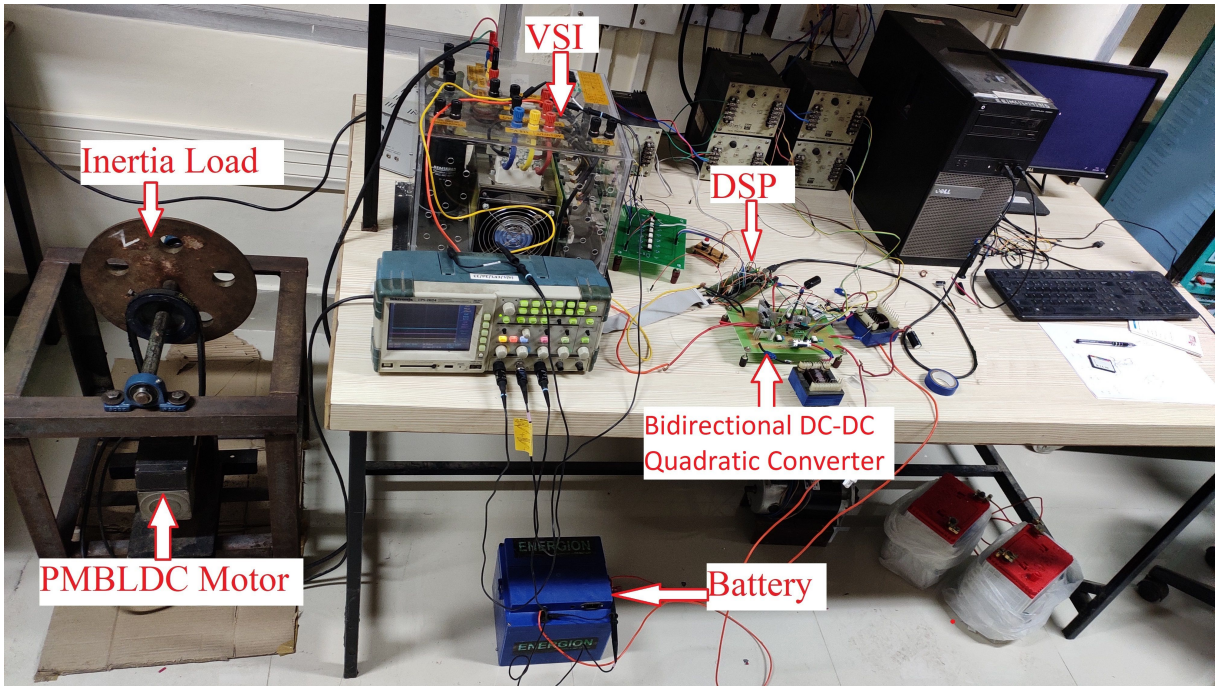

Figure 3.18: Hardware Setup.

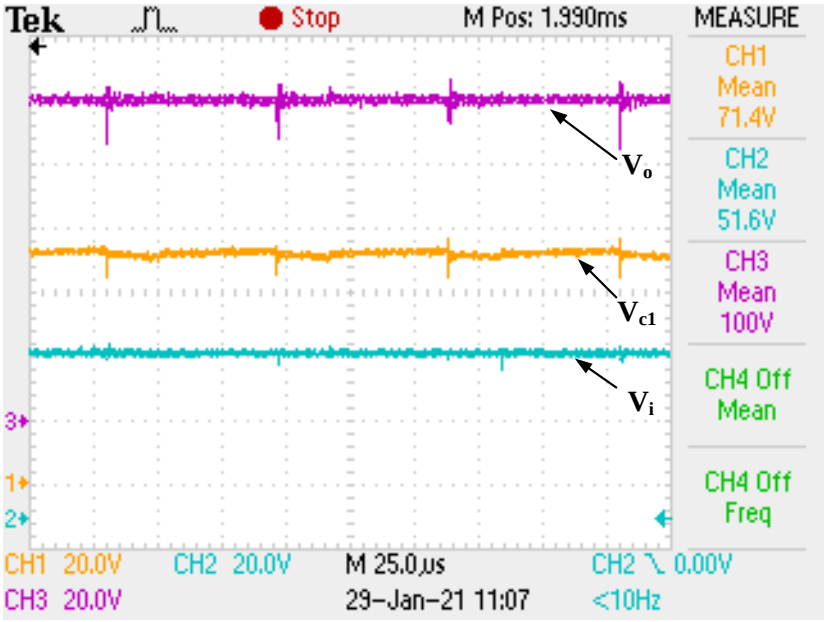

Figure 3.19: System voltages in steady state boost operation of converter; capacitor C_1 (V_{c1}), battery voltage (V_i), and output voltage (V_o).

Figure 3.19 shows different voltages, battery voltage, capacitor voltage, and output voltage in steady state during boost mode operation of the converter at 30 % duty ratio.

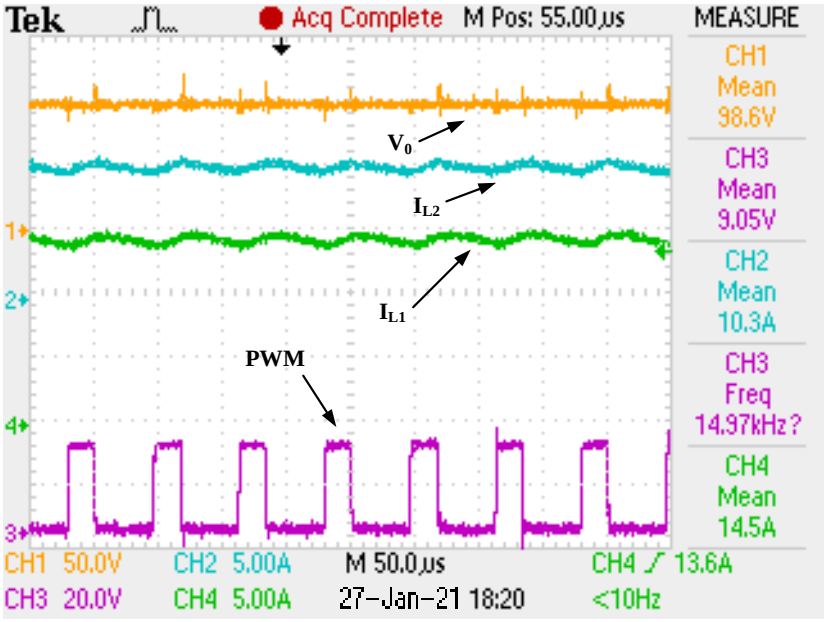

Figure 3.20: Boost mode operation of the converter; output voltage (V_o), I_{L2}, switching PWM, and I_{L1}.

The steady-state inductor currents I_{L1}, I_{L2}, output voltage, and switching PWM are shown in Figure 3.20 for boost mode operation. Both the inductors are charging during the ON time of the switch and discharging during the OFF time.

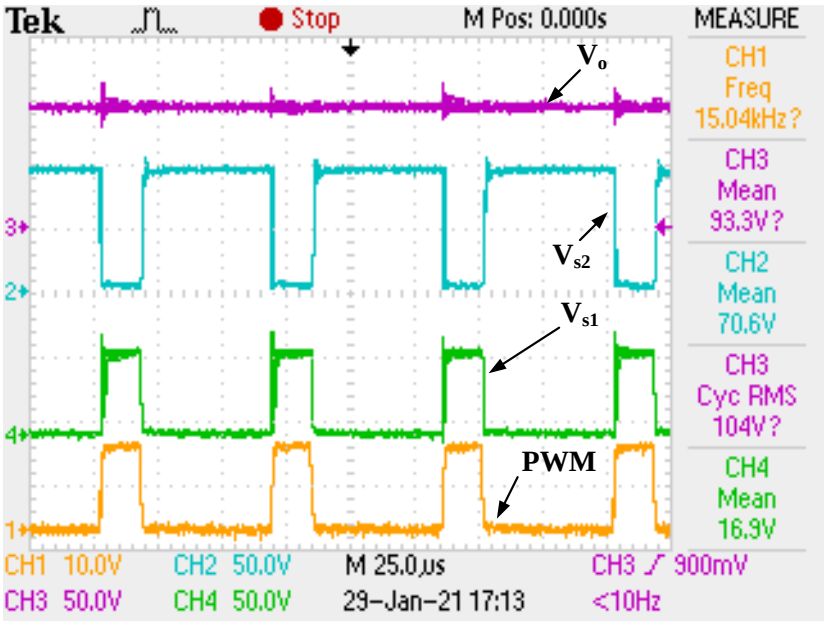

Figure 3.21: Switching PWM, Voltage stress on switches S_1 (V_{S1}), S_2 (V_{S2}), and output voltage (V_o) in boost mode operation of converter

The voltage stress on switches S_1, S_2 and output voltage V_o with switching PWM during the boost mode of the converter are shown in Figure 3.21.

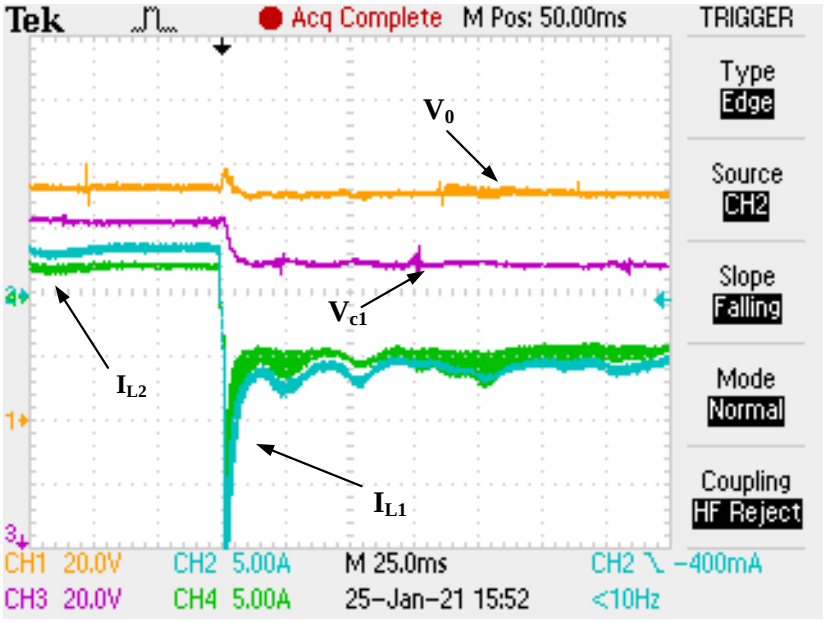

Figure 3.22: Transition of motor from motoring mode to regenerative braking mode; V_{c1} , I_{L1}, V_o, and I_{L2}.

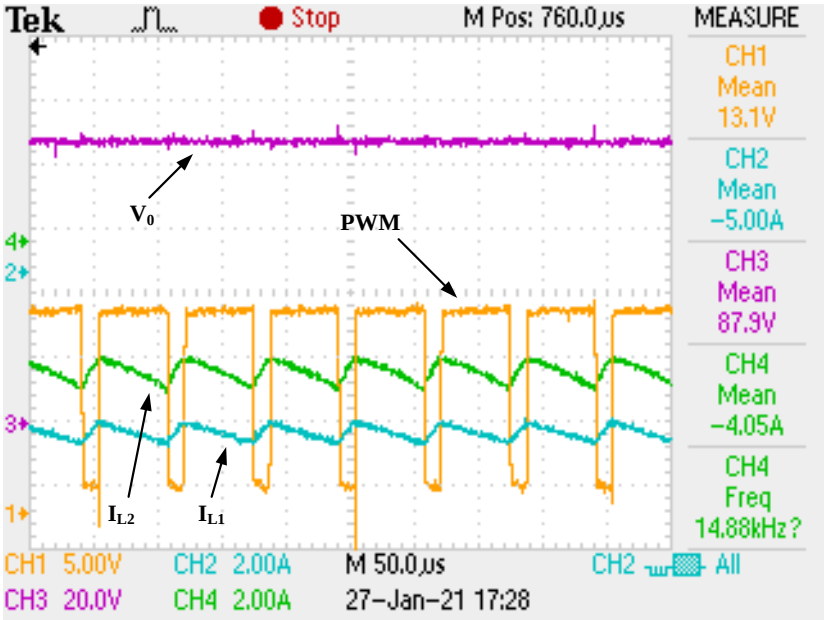

Figure 3.23: Buck mode operation of converter; switching PWM, I_{L1} , V_o, and I_{L2}.

Figure 3.22 shows the transition of the system operation from motoring to the RB mode. The negative currents are indicative of the regenerative mode operation. During

RB, the steady-state inductor currents I_{L1}, I_{L2}, output voltage, and switching PWM are presented in Figure 3.23, aligned with those obtained in the simulation. It indicates the converter operation in the buck mode and the successful energy transfer from the PMBLDC motor to the battery. The value of inductor currents during RB is matched with the simulation result. The continuous charging of the output capacitor due to VSI performing the boosting operation keeps the DC link voltage almost constant during the initial period of the braking process.

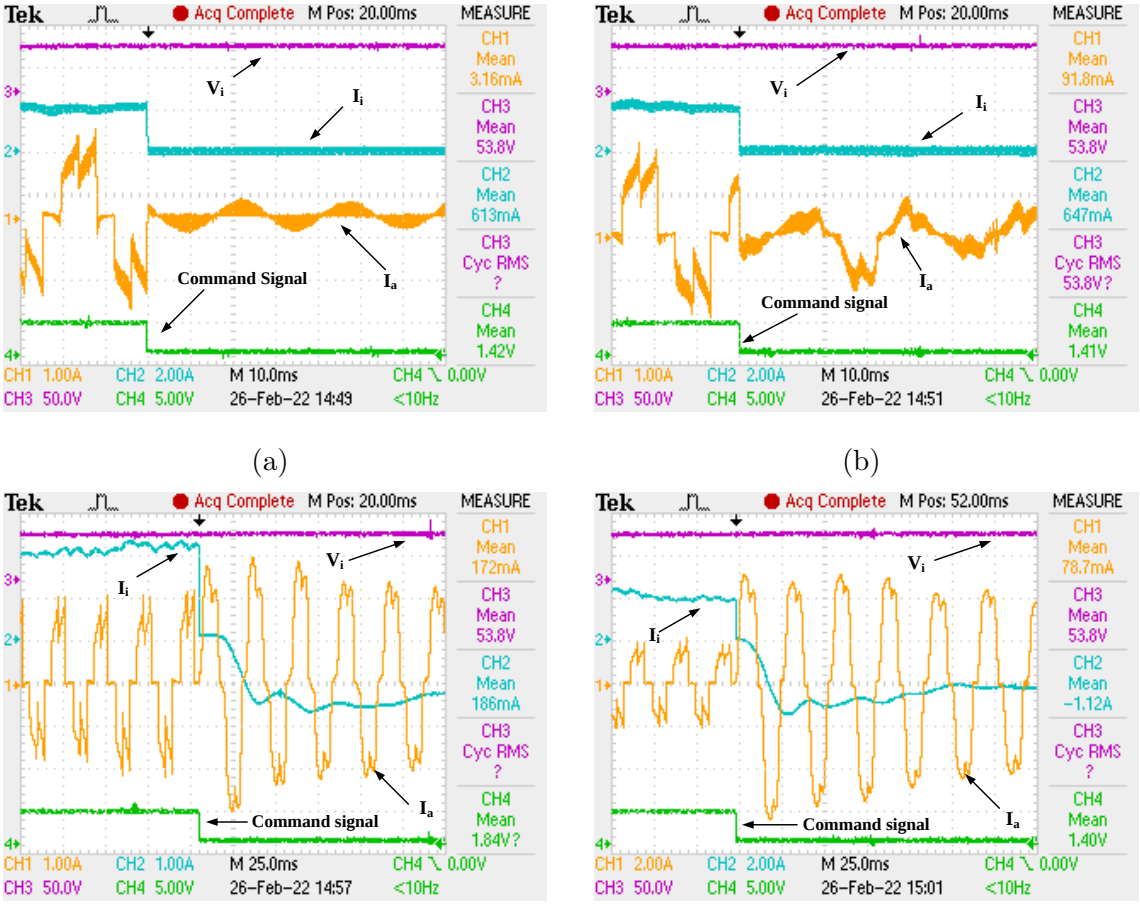

Figure 3.24: Armature current, battery current, battey voltage, command signal at different braking duty (a) $\delta = 0.4$ (b) $\delta = 0.5$ (c) $\delta = 0.6$ and (d) $\delta = 0.7$.

The three-switch control strategy of VSI for RB of PMBLDC motor is done at different braking duty. The braking duty is varied from 0.4 to 0.7, the armature current, battery current, battery voltage, and command signal for RB action are illustrated in Figure 3.24. When the command signal is high, the PMBLDC motor acts in motoring operation and when the command signal goes low, the PMBLDC motor act as a generator

in RB. One can see that as braking duty increases then the armature current, battery charging current, and braking torque increase. The braking duty depends on how much brake force should be applied to the wheel of the EV. The results obtained in experimental is compared with simulation results for validation are done in Table 3.3.The speed of the motor during experiment is measured with stroboscope tachometer. The theorytically obtained efficiency with respect to output power of the converter in boost mode operation is illustrated in Figure 3.25. The comparison of different bidirectional DC-DC converters with the proposed converter are done in Table 3.4.

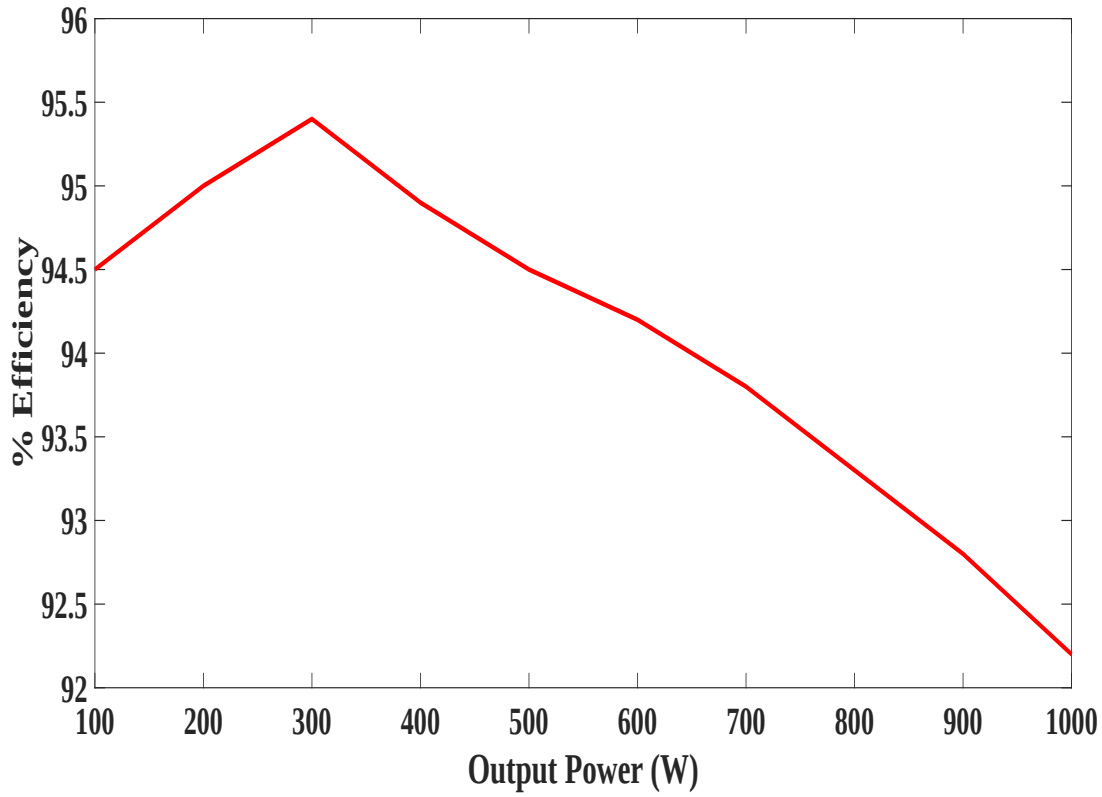

Figure 3.25: The curve between % Efficiency and output Power during boost mode.

Table 3.3: Comparison of simulation and experimental results

Parameters	Output Voltage V_o	Capacitor voltage V_{c1}	Input current I_i	Inductor current	Voltage stress	Motor speed
Simulation	98 V	68.5 V	14 A	I_{L1}=14 A I_{L2}=10 A	V_{s1}=V_{s3}=68.5 V V_{s2}=V_{s4}=98 V	1900 rpm
Experimental	100 V	71.4 V	14.5 A	I_{L1}=14.5 A I_{L2}=10.3 A	V_{s1}=71.4 V V_{s2}=100 V	1850 rpm

Table 3.4: Comparision of different bidirectional converters with proposed converter

Reference	Total components	Voltage ratio boost	Voltage ratio buck	Maximum voltage stress	Maximum Efficiency
Converter in [9]	1 inductor 3 capacitors 4 power switches	$\frac{2}{(1-D)}$	$\frac{D}{2}$	$\frac{2}{(1-D)}$	92.5 %
Converter in [120]	1 Transformer 4 capacitors 4 power switches	$\frac{2n}{1-D}$	$\frac{D}{2n}$	$\frac{2n}{1-D}$	94 %
Converter in [67]	1 Transformer 1 inductor 3 capacitors 6 power switches	$\frac{N}{(1-D)^2}$	$\frac{(1-D)^2}{N}$	$\frac{N}{(1-D)^2}$	95 %
Proposed converter	2 inductors 2 capacitors 4 power switches 2 power diode	$\frac{1}{(1-D)^2}$	D^2	$\frac{1}{(1-D)^2}$	95.4 %

3.7 Conclusion

The QGBC for motoring and RB of PMBLDC motor is designed, developed, and tested in the laboratory. The power flow direction is controlled successfully by changing the working mode of the VSI and the QGBC. The inertial load's mechanical energy is converted to electrical energy during regenerative braking and fed back to the battery, as evident from the results. A control strategy is implemented to boost the back-EMF of the PMBLDC motor by controlling the VSI and using the self-inductance of the motor. The three-

switch strategy is a cost-effective and simple sensorless braking commutation method for an electric vehicle. The implemented strategy and the system configuration proposed in this chapter have shown an economical and practical approach to eliminate the drawbacks of regenerative braking in buck mode of Bidirectional DC-DC converter (BDC).